

Effect of size, proteic composition, and heat treatment on the colloidal stability of proteolyzed bovine casein micelles

Patricia H. Risso · Verónica M. Relling ·
Martín S. Armesto · Miryam S. Pires · Carlos A. Gatti

Received: 10 July 2006 / Accepted: 21 November 2006 / Published online: 19 January 2007
© Springer-Verlag 2007

Abstract The casein micelles of reconstituted nonfat milk that have been fractionated by controlled pore glass chromatography showed a relationship between their size and their proteic composition: The fractions containing the smaller particles were richer in κ -casein than the fractions containing the bigger ones, in accordance with the casein micelle model of submicelles. The initial aggregation rate of micelles of different sizes, partially proteolyzed with chymosin (para-casein micelles), was measured in conditions of enzyme excess in which aggregation is the rate-limiting step of enzymatic coagulation, showing higher rates for the smaller micelles with the production of less compact para-casein micelle networks. This behavior could be explained in terms of electrostatic and steric colloidal stabilization due to their lower negative net charge and size and to a higher surface density of hydrophobic “patches” of proteolyzed κ -casein related to a higher probability of effective collisions between particles. Differences in the β -casein content did not seem to affect the initial aggregation rate of the micelles. On the contrary, the modifications of the micelle surface by heating affected the colloidal stability of the hydrolyzed micelles in different ways. The denaturation of the whey proteins and the formation of covalent complexes with κ -casein modify the micelle sur-

face, increasing specially the steric stabilization, and produces a diminution in the number of hydrophobic sites that could be able to give interparticle hydrophobic interactions.

Keywords Bovine casein micelles · Proteic composition · Size · Colloidal stability · Enzymatic coagulation

Introduction

Caseins (CN), the major protein fraction in bovine milk, occur in the aqueous phase of milk as stable colloidal aggregates known as casein micelles (CM). CM are roughly spherical, fairly swollen particles with a diameter ranging from 80 to 680 nm. The principal proteic components of CM are four kinds of caseins: α_{S1} -, α_{S2} -, β - and κ -casein (α_{S1} -CN, α_{S2} -CN, β -CN, and κ -CN) in a molar proportion of 4:1:4:1.3, respectively [1]. These caseins remain linked together in the CM with the contribution of colloidal calcium phosphate (CCP), a mineral complex involving mainly calcium and phosphate ions [2].

Different structures for the CM have been hypothesized in the last 40 years, mainly on the basis of physico-chemical studies of casein aggregation and electron microscopy of the micelles [3]. The different models proposed for the CM structure could be roughly classified in two general categories, models of subunits and models of internal structure [4]. The former of these categories postulate that CM are made of smaller units called submicelles. Two main types of sub-micelles have been proposed: one primarily consisting of α_S - and β -CN; the other of α_S - and κ -CN. The sub-micelles can be linked together to form CM, mainly through small clusters of calcium phosphate. Those with κ -CN remain preferentially at the CM surface, allowing the hydrophilic molecular

P. H. Risso (✉) · V. M. Relling · M. S. Armesto · C. A. Gatti
Departamento de Química-Física, Facultad de Ciencias
Bioquímicas y Farmacéuticas, Universidad Nacional de Rosario,
Suipacha 531,
2000 Rosario, Argentina
e-mail: phrisso@yahoo.com.ar

M. S. Pires
Departamento de Química Analítica, Facultad de Ciencias
Bioquímicas y Farmacéuticas, Universidad Nacional de Rosario,
Suipacha 531,
2000 Rosario, Argentina

chain of the C-terminal end of the κ -CN to protrude from the CM by preventing (by electrostatic and steric repulsion) the aggregation or further growth of the micelles and stabilizing the CM in aqueous suspension to prevent CM flocculation [5–9]. Furthermore, assuming that caseins are assembled into the micelles by hydrophobic bonds and through the formation of calcium bridges by the CCP and casein phosphoserin residues, the occupation of the micelle surface by κ -CN with only one phosphoserin residue contributes to complete micelle formation, impairing further casein aggregation to the particle [10].

Although the sub-micelles model can reasonably explain different features of CM structure and behavior, there are some observations that do not agree with such a model. Among these discrepancies, some refer to the evidence (obtained by electron microscopy and experiments of casein enzymatic digestion) of the presence of small patches of CCP called nanoclusters that involve serine phosphate groups of the caseins and, probably, also glutamine residues through the CM. This has led Holt [11, 12] to propose another model in which the calcium phosphate nanoclusters form cementing centers from which the CM grow as a tangled web of flexible casein networks forming a gel-like structure. Also in this model, the C-terminal region of the κ -CN extends outside to form a hairy layer, providing electrostatic and steric stabilization for the micelles in aqueous suspension [13–15].

An assumption shared by both kinds of models is that the presence of κ -CN in the CM outer layer limits their growth and determines their size. In the last 20 years or more, it has been supported by different authors based on different technical approaches that higher proportions of κ -CN correspond to the formation of smaller and more solvated micelles [16–18].

Because CM physicochemical properties are closely related to their functional behavior, the chemical composition and size of the micelles may be expected to affect enzymatic coagulation rate and final results. Enzymatic coagulation is a process extensively used in cheese manufacturing, which involves three fundamental stages. In the first one, chymosin, the rennet component with the higher milk clotting activity catalyzed the cleavage of κ -CN at the Phe(105)–Met(106) peptide bond, removing the hydrophilic moiety of the protein from the CM surface and producing, thereby, the destabilization of the micelles. These partially hydrolyzed micelles known as para-casein micelles (pCM) aggregate spontaneously in the second step of the enzymatic coagulation to form (at an adequate casein concentration) a viscoelastic gel or curd. The rearrangement of the inter-particle interactions in the gel network during the third step of the process leads to the shrinkage of the gel with the drainage of a part of the serum enclosed in it (syneresis) [19–22]. Several authors have studied the relationship between MC size and proteic

composition, intimately related to size and enzymatic coagulation rate [23–26].

Although the results obtained could be contradictory, it may be taken into account that the methods used to evaluate the coagulation time measured the rate of the different steps of the process. Whereas some methods considered only either the proteolysis or the aggregation stage, others measured the global time until the apparition of visual aggregation or viscoelastic changes that indicate the gel formation. However, some of the authors mentioned before agree with the following observation: Smaller CM produce firmer and more compact curds, a fact that could be important for cheese texture and quality.

CM, on the other hand, are usually submitted to heat treatments of different intensity during milk processing. These heat treatments are usually carried out at temperatures high enough to produce structural changes in CM surface because of the heat denaturation of the whey proteins (β -lactoglobulin, α -lactalbumin, etc.) and complex formation with the caseins, especially surface κ -CN, via the formation of intermolecular disulfide bridges and, perhaps, other less specific forms of interactions such as hydrogen bonding and electrostatic interactions between opposite charges [27, 28].

Although this interaction of the denatured whey proteins with CM could be potentially interesting as a way to recover these proteins in cheese, it must be considered that the CM surface modification also produces changes in the rate of the coagulation process and in the final cheese quality [29, 30].

The aim of this work was to gain insight on the effects that changes in CM size and proteic composition, as well as CM heat treatments, have on the enzymatic coagulation rate, especially in the aggregation step of pCM, and on the final structural properties of the curds obtained.

Experimental sections

Materials and methods

Casein micelles suspensions

The reconstituted casein micelles (RCM) suspension was prepared from commercial nonfat dried milk (MOLICO, Société des Produits Nestlé SA, Vevey, Switzerland) reconstituted to 10% (w/v) in 5-mM CaCl_2 (Merck, Germany). The suspension of CM modified by heat treatment (HCM) was obtained by heating the RCM suspension at 90 °C for 10 min with continuous stirring, then by cooling it at room temperature and by filtering it, firstly, through filter paper and then through a Whatman GF/A glass fiber filter (1.6- μm pore) to retain precipitate denatured whey proteins and

remnant fat globules [31]. Sodium azide (Mallinckrodt Ch. W., New York, USA) was added in all the cases at the rate of 0.01–0.02% w/v as a preservative, and both suspensions were held 24 h at 4 °C before use.

The RCM and HCM dilutions in the different buffers used were prepared from their concentrated suspensions that were previously equilibrated at room temperature. The dilutions were maintained in a water bath at working temperature until constant turbidity (τ) values to confirm that the association/dissociation equilibrium of the micelles in the different conditions has been reached.

Exclusion chromatography on controlled pore glass

Chromatography on controlled pore glass (CPG) was used to separate RCM from the free caseins and whey protein remnants in the solution, and to obtain fractions of micellars in different sizes. The rapid flow that is possible to develop in such porous rigid matrix produces a good resolution in short running times, contributing in this way to minimize micelle dissociation during the chromatographic run [32]. CPG-10 (300-nm mean pore diameter, 120/200 mesh size, Sigma Chemicals, St. Louis, USA) was cleaned by treatment with 5% w/v HNO₃ (Cecarelli, San Lorenzo, Argentina), 1 h at 90 °C [33], washed thoroughly with distilled water, and held for 24 h in three-column volumes of 1% w/v PEG 20,000 (Sigma Chemicals) [34]. Before each chromatographic run, the CPG was allowed to equilibrate for 24 h with three-column volumes of the elution buffer Tris-HCl at 10 mM (Sigma Chemicals), CaCl₂ at 10 mM, PEG 20,000 at 0.4% w/v, sodium azide at 0.02% w/v, and pH 6.4. The column dimensions were 1.6×144 cm. The chromatographic conditions were 20–30 °C and a flow rate of 2.5 ml min⁻¹. Fractions of 1.0 or 2.0 ml were obtained according to their posterior use. The fractions were identified as RCM_i, where *i* was its correspondent order number in the elution. The protein concentration of the fractions was determined by their absorbance at 280 nm, corrected for the turbidity calculated by the extrapolation of log absorbance vs log wavelength plots obtained in the 400- to 700-nm range.

The casein concentration of the fractions was measured by Kuaye's method [35].

Urea–sodium dodecyl sulfate–polyacrylamide gel electrophoresis

The proteic composition was studied by urea–sodium dodecyl sulfate–polyacrylamide gel electrophoresis (Urea–SDS–PAGE) according to the method of Laemmli [36, 37], using a vertical gel system. Thirty-microgram protein samples were dissolved in 1 mL of buffer containing 0.1-M Tris-HCl, pH 6.8, 2% (w/v) SDS (Merck), 10% (v/v) β -mercaptoethanol (BDH Chemicals, Poole, England), 10% (v/v) glycerol

(Merck), and 0.01% (w/v) Coomassie Brilliant Blue R250 (Fluka, St. Gallen, Switzerland). The separating gel was composed of 20% (w/v) acrylamide (Sigma Chemicals) and 0.53% (w/v) bis acrylamide (Sigma Chemicals) dissolved in 0.38-M Tris-HCl buffer pH 8.8 containing 7- to 9-M urea (Merck) and 0.5% (v/v) SDS. The stacking gel was composed of 7.5% (w/v) acrylamide and 0.16% (w/v) bis acrylamide dissolved in 0.12-M Tris-HCl buffer pH 6.8 containing 0.1% (v/v) SDS. Migration was run for 2 h at 25 °C and under 100-V constant voltage conditions.

Proteins were stained with 0.1% (w/v) Coomassie Brilliant Blue R250, 45% (v/v) methanol (Cecarelli), and 10% (v/v) acetic acid (Cecarelli) staining solution, and destained with 10% (v/v) methanol and 10% (v/v) acetic acid destaining solution. The relative intensity of the stained bands was determined by the scanning of the stained gels and the analysis of the pixel densities of the digitized protein bands using software specially designed for this purpose (X-Gel). Deconvolution of the scanning pattern curves was performed when necessary by means of the GRAMS program. The protein bands were identified using commercial α _S-, β -, and κ -CN (Sigma Chemicals). These same standards were used not only to determine the range of protein concentrations at which the relationship between pixel density and concentration remains linear but also the reproductiveness of the method.

Changes in size and compaction of RCM, HCM, and RCM_i

Micelle changes in size and compaction were followed using the wavelength (λ) dependence of the τ in the 400- to 700-nm range, where the absorption due to the protein chromophors is negligible. For monodispersed particles of molecular weight *M*, concentration *c*, and with a refractive index close to that of the solvent, the turbidity is given by:

$$\tau = HcMQ, \quad H = \frac{32 \pi^2 n_0^2 \left(\frac{dn_1}{dc}\right)^2}{3 N \lambda^4}, \quad (1)$$

where n_0 and n_1 are the refractive indexes of the pure solvent and the solution, respectively, *N* is the Avogadro's number, and dn_1/dc is the specific refractive index increment. The dissipation factor *Q* results from the internal interference of light scattered by the particle at all the angles θ and is incorporated to the expression when the particles are bigger than the incident λ . The function *Q* depends on the particle size and can be defined as:

$$Q = \frac{3}{8} \int_0^\pi P(q, R) (1 + \cos^2 \theta) \sin \theta d\theta, \quad (2)$$

where θ is the dispersion angle of light and *P*(*q*, *R*) is a size factor function of the wavelength vector *q* and the radio *R* of the particle [38].

Simulation studies using different models for particle aggregation have highlighted the fractal nature of the colloidal aggregates obtained [39]. For an object with fractal structure, the expression for Q takes the form:

$$Q = \frac{3}{8} \int_0^\pi P(q, R) S(q) (1 + \cos^2 \theta) \sin \theta d\theta, \quad (3)$$

where $S(q)$ is a structure factor that describes the spacial arrangement of the dispersion elements or monomers within the aggregate [40].

From Eq. 1, we can obtain at constant c the derivate:

$$\frac{d \log \tau}{d \log \lambda} = \frac{d \log Q}{d \log \lambda} + 2 \frac{d \log (n_{\text{dc}})}{d \log \lambda} - 4 = \beta + \gamma - 4. \quad (4)$$

The parameter β is then related to the size, shape, and compaction degree of the particles, and it can be used to detect changes in micelles submitted to different conditions.

Taking into account that the different micelle samples to be studied are not monodispersed, τ will be a function of the weight average of the molecular weight (\overline{M}_w) and of the z average of the dissipation factor (Q_z) that depends on the size distribution of the particles:

$$\tau = H \overline{M}_w Q_z \quad (5)$$

From Eq. 5, it is possible to find the direct relationship between β and the weight diameter average of the CM [41].

Assuming an estimated value of -0.2 for γ for proteins in the range of 400 to 800 nm, β can be calculated from the slope of $\log \tau$ vs $\log \lambda$ plots in such λ range, applying the following relation:

$$\beta = 4, 2 + \frac{\partial \log \tau}{\partial \log \lambda} = 4, 2 + \frac{\partial \log A}{\partial \log \lambda} \quad (6)$$

τ was measured as the absorbance using a Jasco V-550 spectrophotometer for measurements at one λ or a diode array Spekol 1200 spectrophotometer for instantaneous spectra determination, pouring 3 mL of the micelle suspension samples into a 1-cm spectrophotometer cuvette in a jacketed cuvette holder at a temperature maintained by water circulation.

To verify if β was actually related to the average size of the particles, the micelle size distribution functions (SDF) and the average $D_{6,5}$ diameters of all the samples were determined by dynamic light scattering (DLS) using a Brookhaven BI-2005 M equipment with a He-Ne laser ($\lambda_0 = 632.8$ nm) with a maximal power of 15 mV, and using 90° as the measuring angle during 420 s for each of the three determinations for each sample. $D_{6,5}$ was determined by applying the method of cumulants [42], and the SDF was calculated by using the Matlab program [43]. Measurements at several scattering angles were used in some cases to detect the presence of small populations of big size

particles and bimodality in the samples. The diluted micelle samples in the correspondent buffer that had previously been filtered through a Millipore of 1- μm pore diameter to eliminate dust particles were transferred to glass cuvettes in a jacketed cuvette holder immersed in decaline (bicyclo [4.4.0]-decane) and maintained at the desired temperature by a MGW LAUDA RC3 circulation bath. The buffer viscosity and refractive index (n_m) were 7.23×10^{-3} g $\text{cm}^{-1} \text{s}^{-1}$ and 1.3316, respectively. The refractive indexes of the particles were measured using the method of Ambrose Griffin and Griffin [44].

On the other hand, it has been shown that β , for a system of aggregating particles of the characteristics of CM, tends, upon aggregation, towards an asymptotic value that can be considered as a fractal dimension (D_f) of the aggregates.

Enzymatic coagulation studies

The second step of the CM enzymatic coagulation, i.e., the pCM aggregation, starts when 60–85% of the surface κ -CN has been proteolyzed by the enzymatic action exerted by the chymosin, the enzymatic rennet component that is able to act specifically on κ -casein in the times at which the enzymatic coagulation was produced in our working conditions [45, 46]. Therefore, this step is usually overlapped with the end of the first one. However, the second step can be practically isolated by working with enzyme excess to complete the κ -CN proteolysis as soon as possible at the beginning of the process. Under these conditions, the pCM aggregation appears as the rate-limiting step of the coagulation [20, 46, 47]. The concentration of rennet necessary to produce the maximal proteolysis of κ -casein in a time practically negligible compared to the pCM aggregation time was determined following the release of the hydrophilic κ -CN moiety, known as caseinomacropetide (CMP), as a function of time. One hundred microliters of a 1/8 (v/v) dilution of standard Hansen's liquid rennet in distilled water were added to 3 mL of a 1/100 (v/v) dilution of RCM, HCM, or RCM_i in the correspondent buffer, previously equilibrated at 35 °C for 2 h. After selected times, the reaction was stopped by the addition of 3% (w/v) trichloroacetic acid and centrifuged for 5 min at $12,000 \times g$ [48]. The CMP were determined in the supernatants by Lowry–Peterson's method, and their concentration was expressed as the absorbance at 750 nm [49]. The standard Hansen's liquid rennet was a gift of COTAR SA (Argentina, Rosario) with a milk-clotting activity of 0.03 RU, where 1 RU is the required activity for rennet in 100 s; 10 ml of dried milk suspension reconstituted in 10-mM CaCl_2 at nonadjusted pH (approximately 6.4) and in IDF standard 110A:1987 specified conditions.

In the conditions of rennet excess, the pCM aggregation kinetics can be studied by estimating the initial rate of

doublet formation, as proposed by Smoluchowski for Brownian aggregation [46, 50], from the measurement of β changes as a function of time. Three-milliliter samples of RCM, HCM, or RCM_i 1/100 (v/v) dilutions in 10-mM Tris-HCl, 10-mM CaCl₂, at pH 6.4 were allowed to equilibrate at 35 °C for 24 h. The equilibrated samples were poured into spectrophotometer cuvettes in a jacketed cuvette holder maintained at 35 °C by water circulation, in a Jasco V-550, or a diode array Spekol 1200 spectrophotometer. Enzymatic coagulation was started by the addition of 100 μ L of a 1/8 (v/v) rennet dilution in distilled water. The mixture was gently stirred with a Teflon stirrer for 5 s, and its absorbance spectra between 400 and 700-nm were recorded as a function of time until a maximal and constant A value was reached. The values of β during the coagulation were calculated, and the initial slope of β vs time plots, $(\partial\beta/\partial t)_0$, was used as an estimation of the initial aggregation rate [45]. The D_f of the aggregates was estimated from the β vs t plots as the maximal value of β reached.

Statistical analysis

Data were reported as mean value \pm standard deviations for all data points. All the experiments were carried out three times at least. A standard ANOVA analysis was used to determine significant differences between variables.

In the correlation analysis, the strength of the linear relationship between the values of β_0 and the average $D_{6,5}$ for RCM, HCM, and RCM_i were calculated using the Pearson coefficient of correlation r . The statistical significance was considered at p values below 0.05.

Results and discussion

State of RCM_i

Figure 1 shows the elution patterns obtained in the CPG chromatography of RCM expressed as the RCM_i concentration or the RCM_i average $D_{6,5}$ diameter in the function of the fraction number.

The values of τ , β , and average $D_{6,5}$ obtained for the RCM_i characterization are reported in Table 1.

τ_0 and β_0 are the values obtained for the RCM_i with their concentration previously adjusted to 0.30 g l⁻¹ with a buffer of 10-mM Tris-HCl and 10-mM CaCl₂ at pH 6.4 and 35 °C. Because the samples were diluted in the working buffer to obtain the concentration required by the photon counting rate for DLS measurements, it was previously verified that such dilution produced only negligible variations in the micelles' average size. In fact, for 1/10 dilution the variations observed were in the range of only 5–8 nm.

The RCM_i average $D_{6,5}$ diameter determined by DLS showed a good linear correlation ($r=0.96$; $p<0.05$) with the

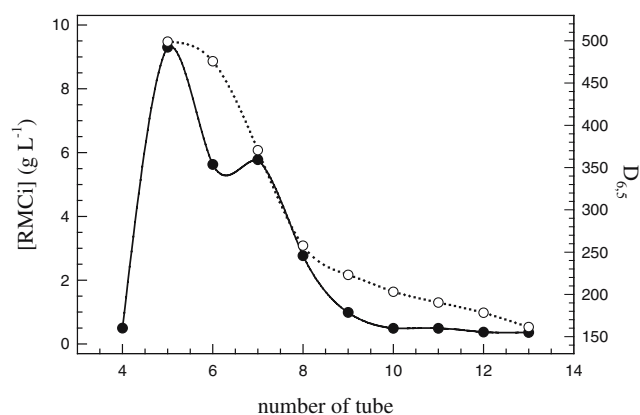


Fig. 1 Chromatography on controlled pore glass elution patterns of different fractions of the reconstituted casein micelles (RCM_i) in function of the RCM_i concentration (filled circle) or RCM_i average $D_{6,5}$ diameter (open circle). Each point is the average of three independent determinations

values of β_0 obtained for these fractions (Fig. 2), allowing us to assume that the parameter β can be used to estimate the average size of the particles in fractions of similar composition.

The shape of the elution patterns in Fig. 1 shows that the RCM samples presented polydispersity with higher concentrations for the bigger particles. The average $D_{6,5}$ values determined for each of the RCM_i, even for those of small particles present in low concentration, were always within the range of values that correspond to well-defined micelles.

The observation of the PAGE patterns obtained for different chromatographic fractions (Fig. 3) showed that the κ -CN content increased when the size of the RCM decreased with simultaneous reduction in the content of the others caseins.

These results are coherent with studies on the proteic composition of CM fractionated by different methods [51].

Table 1 Characteristic parameters of reconstituted casein micelles (RCM_i): turbidity (τ_0) as absorbance at 600 nm, parameter β_0 , and average size $D_{6,5}$

RCM _i	τ_0 ($A_{600 \text{ nm}}$)	β_0	$D_{6,5}$ (nm)
RCM ₅	0.2732	1.4690	498.9
RCM ₆	0.2977	1.547	475.8
RCM ₇	0.2616	1.487	370.5
RCM ₈	0.1544	1.278	257.5
RCM ₉	0.1910	1.371	223.0
RCM ₁₀	0.1806	1.394	202.9
RCM ₁₁	0.1141	1.2880	190.2
RCM ₁₂	0.1587	1.2930	178.1
RCM ₁₃	0.0873	1.181	161.2

RCM_i concentration of 0.30 g l⁻¹ in a buffer of 10-mM Tris-HCl, 10-mM CaCl₂ at pH 6.4 and a temperature of 35 °C

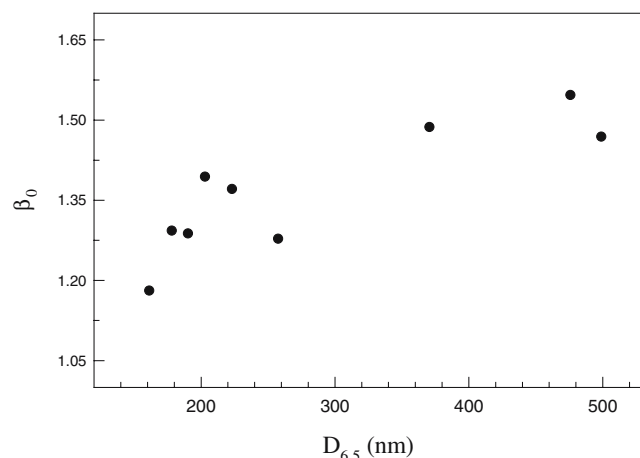


Fig. 2 Correlation between the values of parameter β_0 and the average $D_{6,5}$ diameter for the reconstituted casein micelle fractions (RCM_i) ($r=0.96$; $p<0.05$)

RCM, HCM, and RCM_i enzymatic coagulation

The enzymatic coagulation of the different kinds of micelles and micellar fractions was studied using rennet concentrations at which the pCM aggregation acts as the limiting rate step. The proteolytic step was maintained within times of 10 s in all the cases.

As it can be seen in Fig. 4, as an example for RCM, the enzyme/substrate concentration ratio used allows the first step to be completed (as shown by the CMP release) practically before the start of the aggregation step, followed by the τ increment in the function of time.

Figure 5 shows the enzymatic coagulation of RCM_i followed by the τ and β values as functions of time. The comparison of the behaviors of both parameters showed that the smallest particles reach maximal τ values and tend to reach the D_f (maximal β value) faster than the bigger particles.

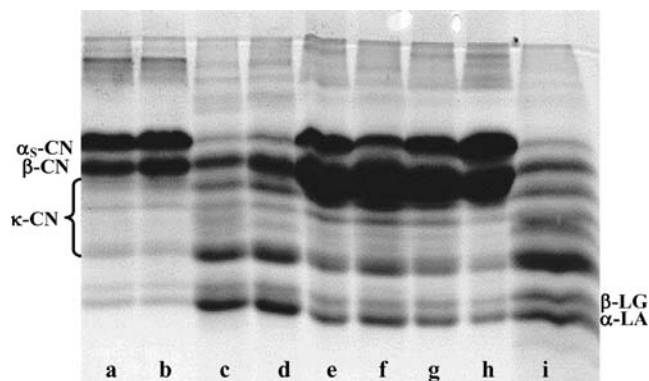


Fig. 3 Urea-SDS-PAGE of the different fractions obtained for the molecular exclusion chromatography on controlled pore glass of the reconstituted casein micelles (RCM_i); elution buffer of 10-mM Tris-HCl, 10-mM $CaCl_2$, 0.04% w/v PEG 20,000, pH 6.4; temperature of 25 °C; flow rate of 2.5 ml/min. **a** and **b** Caseinates, **c** RCM_{11} , **d** RCM_{10} , **e** RCM_8 , **f** RCM_7 , **g** RCM_6 , **h** RCM_5 , **i** RCM_{13} ; β -LG β -lactoglobulin, α -LA α -lactalbumin

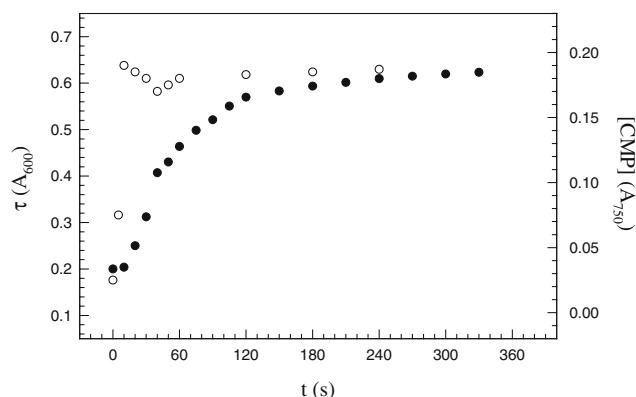


Fig. 4 CMP release and RCM flocculation by action of rennet as function of the time. Filled circle, τ as A at 600 nm; Open circle, CMP concentration as A at 750 nm. CN Concentration 0.3 g L^{-1} in a buffer of 10-mM Tris-HCl, 10-mM $CaCl_2$, pH 6.4; temperature of 35 °C, rennet of 100 μL of 1/8 v/v dilution. Each point is the average of three independent determinations

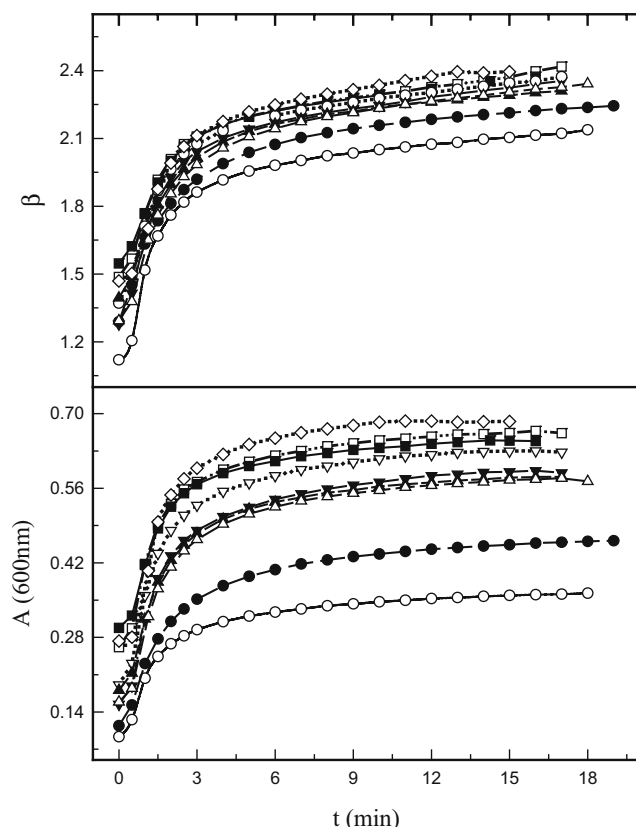


Fig. 5 Enzymatic coagulation of the reconstituted casein micelles fractions (RCM_i) followed by the parameter β (**a**) and turbidity (τ) measured as A at 600 nm (**b**) as functions of the time. RCM_{13} (open circle), RCM_{12} (filled circle), RCM_{11} (open triangle), RCM_{10} (filled triangle), RCM_9 (inverted open triangle), RCM_8 (inverted filled triangle), RCM_7 (open square), RCM_6 (filled square), RCM_5 (diamond). CN concentration 0.3 g L^{-1} in a buffer of 10-mM Tris-HCl, 10-mM $CaCl_2$, pH 6.4; temperature of 35 °C, rennet of 100 μL of 1/8 v/v dilution. Each point is the average of at least two independent determinations

An inverse relationship between the initial aggregation rate, estimated as the maximal value of $\partial\beta/\partial t$, and the initial RCM_i size, estimated through β_0 or using the average $D_{6,5}$, can be observed in Fig. 6.

The kinetic mechanism of doublet formation by the collision of two spherical particles moving by Brownian motion involves, according to the von Smoluchowski model for unstable colloid coagulation, two steps: the diffusion of each of them to the other and the reaction when they are in contact. When the diffusion step is slower than the reaction one, the global rate of the process will be determined by the diffusion rate, and the process can be considered as a diffusion-limited aggregation (DLA) [52]. Different authors have verified that the pCM aggregation can be interpreted by this aggregation model, and that the initial formation of doublets follows a second order kinetics [53]. In the case of rigid, homogeneous spherical particles without any repulsive potential between them, the second order aggregation rate kinetic constant will reach its

maximal value, independent of the particle size, which is known as *rapid* DLA. In the case of pCM, although the cleavage of the CMP reduces their repulsive potentials enough to allow the aggregation to occur, there remains a residual repulsive interaction including both electrostatic and steric components [54]. Under these conditions, pCM aggregation appears as a case of *slow* DLA, and its kinetic constant, lower than that of the rapid DLA, could depend on the particle size and other particle parameters. In our case, as the PAGE results showed, the smaller the RCM_i, the higher their κ -CN proportion. Taken into account the charge contribution of each of the casein kinds, the smaller RCM_i will have lower negative net charge than the bigger ones. Moreover, the loss of the C-terminal moiety of κ -CN by rennet proteolysis contributes to the further reduction of the para-RCM_i (pRCM_i) negative net charge. The theoretical interpretations of colloidal stability applying the Derjaguin, Landau, Verwey and Overbeek theory (DLVO) theory in the case of electrostatic stabilization and the model of Flory and Huggins for the behavior of polymer solutions in the case of steric stabilization [15] allow us to expect a stability decrease for decreases in both the negative pRCM_i charge and the pRCM_i size, which agree with our experimental results. Furthermore, the smaller pRCM will have higher surface density of hydrophobic “patches” of para- κ -CN, leading to an increase of the effective collision probability.

Although β did not reach clearly constant maximal values during the experimental time that could be interpreted as D_f values for any of the RMC_i, Fig. 5 shows a tendency to reach higher β values for the fractions containing bigger particles. Thus, RCM₅ and RCM₆ reached β values near 2.4, whereas fractions as RCM₁₂ and RCM₁₃ showed almost constant β values about 2.0–2.1 in similar aggregation times. This could be indicating that the smaller micelles tend to produce initially less compact pCMs networks, a behavior probably related to their higher aggregation rate. A similar relationship between coagulation rate and coagula compaction has been observed in the case of the acid coagulation by Braga et al. [55] for gels obtained by fast acidification. On the other hand, different authors have adjudicated the formation of more compact curds to the smaller CM [18, 25]. This apparent contradiction could be related to the fact that the CM network initially formed by pCM in the aggregation step of enzymatic coagulation undergoes structural changes leading to the shrinkage of the gel and the syneresis by rearrangement of the inter-particle interactions in the following step of the process. Therefore, the compaction degree of the curd could depend on the moment of the process at which it was determined.

The aggregation behavior of RCM (average $D_{6,5}$, 237 nm) and HCM (average $D_{6,5}$, 248 nm) was compared

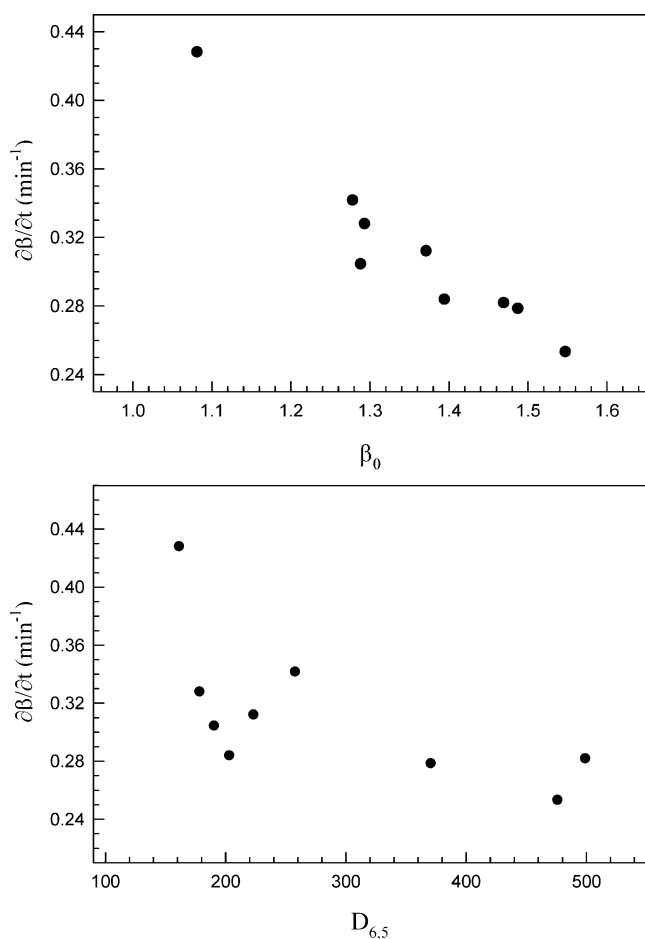


Fig. 6 RCM_i aggregation rate estimated as the maximum $\partial\beta/\partial t$ value as function of parameter β_0 (a) or average diameter $D_{6,5}$ (b). CN concentration of 0.3 g L⁻¹ in a buffer of 10-mM Tris-HCl, 10-mM CaCl₂, pH 6.4; temperature of 35 °C, rennet of 100 μ L of 1/8 v/v dilution. Each point is the average of at least two independent determinations

with that of RCM_i of similar average size, using the fractions RCM_8 (average $D_{6,5}$, 257.5 nm) and RCM_9 (average $D_{6,5}$, 223.0 nm) for this purpose. The PAGE patterns in Fig. 7 allow us to observe the differences in proteic composition of such samples.

The comparison of the samples of whole CM (heated or not) with the fractions obtained by CPG chromatography showed a reduction in the β -casein content for the latter in relation with the casein content of whole caseinates. In the case of HCM, the observed loss in whey proteins can be due to their denaturation and partial precipitation as a consequence of the heat treatment.

Figure 8 shows the aggregation curves for the samples of similar casein concentration of the different kinds of CM of similar initial size. In spite of the differences in β -CN content observed between the RCM and the CPG chromatographic fraction RCM_8 and RCM_9 , the values of their initial aggregation rate were rather similar (0.284 and 0.312 min^{-1} , respectively), a fact that could be indicating that β -CN did not play a determinant role in the aggregation mechanism.

Otherwise, the HCM aggregation behavior was quite different from that of the other micelle samples, showing a clearly lower initial aggregation rate. As described in the Introduction, the heating of milk at 90 °C produces size and structural changes in the CM, especially on their surface, by the complex formation between denatured whey proteins and κ -CN. Thus, the micellar surface becomes ragged, forming many appendages and increasing the thickness of the surface “hairy” layer [29], producing an increase of colloidal stability, especially in its steric component [54]. Apart from this, the surface κ -CN complexed with β -lactoglobulin is not longer accessible to chymosin, producing, thereby, a reduction in the number density of hydrophobic para- κ -CN sites in the micellar surface, a fact that could be associated to a less probability to have effective collisions via the formation of hydrophobic bonds.

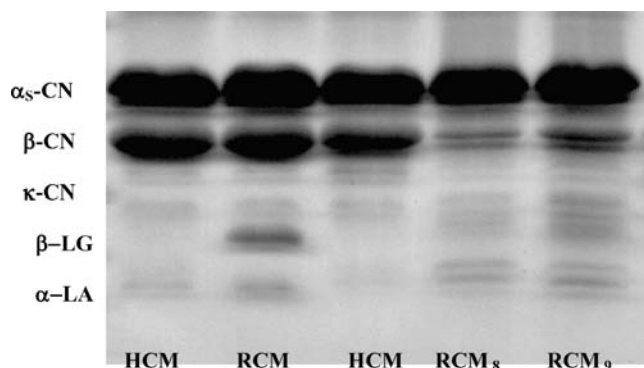


Fig. 7 Urea-SDS-PAGE of the different samples of CM with similar average size. *RCM* Reconstituted casein micelles, *HCM* casein micelles modified by heat treatment, *RCM₈* and *RCM₉* fractions of RCM obtained by CPG, β -LG β -lactoglobulin, and α -LA α -lactalbumin

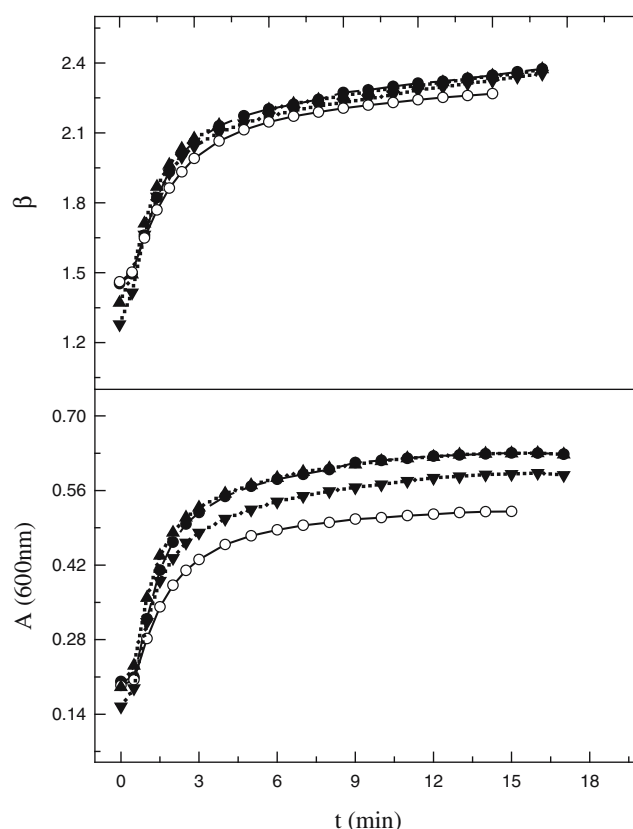


Fig. 8 Enzymatic coagulation of the different samples of RCM with similar average size followed by the parameter β (a) and τ measured as A at 600 nm (b). *RCM₉* (filled triangle), *RCM₈* (inverted filled triangle), *RCM* (filled circle), *HCM* (open circle). CN concentration 0.3 g L^{-1} in a buffer of 10-mM Tris-HCl, 10-mM CaCl_2 , pH 6.4; temperature of 35 °C, rennet of 100 μL of 1/8 v/v dilution. Each point is the average of at least two independent determinations

Conclusions

The CPG chromatographic fractionation of the RCM showed that the average size of the micelles was related to their proteic composition. The fractions of the smaller particles contained a higher proportion of κ -CN, a fact that agrees with the model of submicelles proposed by Slattery and Evard [56], modified in several opportunities by different authors and deeply discussed recently by Walstra [6].

Measurements in enzyme/substrate concentration ratios at which the aggregation is the limiting step of the coagulation rate showed that the micellar size conditions the aggregation rates. In fact, the smaller the micelles, the higher the aggregation rate. This result, which could be contradictory with respect to the results reported by others authors, can, however, be explained by the lower net negative charge of this kind of micelles and their smaller size that diminished the electrostatic and the steric colloidal stability, respectively. Furthermore, the probability of effective collisions between hydrolyzed micelles is also increased for the higher content of surface para- κ -CN.

Comparisons between RCM and RCM_i indicated that the β -CN did not play a decisive role in the aggregation process during enzymatic coagulation.

The modifications of the micelle surface by heating affected the colloidal stability of the hydrolyzed micelles in different ways. The complex formation between whey proteins and κ -CN increased the steric component of the colloidal stability and diminished the surface density of hydrophobic “patches” because of the reduction in the number of surface κ -CN molecules accessible to chymosin. If hydrophobic interactions between such kind of sites played a role in the formation of interparticle bonds in coagulation [57], this diminution of their surface density would be reflected in a decrease in the number of effective collisions between particles and, thus, in a decrease of the aggregation rate, contributing to a higher colloidal stability of the micelles.

These results give evidences of the importance of the participation of hydrophobic interactions in the aggregation step of the enzymatic coagulation process.

Acknowledgment This work was supported by grants from the National University of Rosario (Argentina) and the PICT 09-12651 (BID 1201/OC-AR) of the National Agency for the Scientific and Technological Promotion (Argentina).

The authors would like to thank Bioq. Hebe Botai and Lic. Est. Mercedes Leiva for their technical assistance in the statistical analysis, and also to Marcela Culasso, Susana Spirandelli, and Maria Robson for their assistance in the language correction.

References

- Walstra P, Jenness R (1984) In: Acibia SA (ed) Dairy chemistry and physics. Zaragoza, pp 1–225
- Holt C (1998) J Dairy Sci 81:2994
- Dalgleish DG, Spagnuolo PA, Goff HD (2004) Int Dairy J 14:1025
- Mc Mahon DJ, Mc Manus (1998) J Dairy Sci 81:2985
- Qi PX, Brown EM, Farrell HM Jr (2001) Trends Food Sci Technol 12:339
- Walstra P (1999) Int Dairy J 9:189
- Aoki T (1991) Cross-linkage between casein and colloidal calcium phosphate in bovine casein micelles. In: Parris N, Barford R (eds) Interactions of food proteins, ACS symposium series 454. American Chemical Society, Washington, DC
- Mora-Gutierrez A, Kumosinski TF, Farrell HM Jr (1997) J Agric Food Chem 12:4545
- Farrell HM Jr, Qi PX, Brown EM, Cooke PH, Tunick MH, Wickham ED, Unruh JJ (2002) J Dairy Sci 85:459
- Horne DS (2002) Curr Opin Colloid Interface Sci 7:456
- Holt C, Davies DT, Law AJ (1986) J Dairy Res 53:557
- Holt C, Horne DS (1996) Neth Milk Dairy J 50:85
- de Kruif C (1999) Int Dairy J 9:183
- Tuinier R, de Kruif CG (2002) J Chem Phys 117:1290
- Hunter RJ (1995) Foundations of colloid science, vol I. Oxford Science, Belfast
- Mc Gann T, Donnelly W, Kearney R, Buchheim W (1980) Biochim Biophys Acta 630:261
- Anema SG, Creamer LK (1993) J Dairy Res 60:505
- Gutiérrez-Adán A, Maga EA, Meade H, Shoemaker CF, Medrano JF, Anderson GB, Murray JD (1996) J Dairy Sci 79:791
- Walstra P, van Vliet T (1986) Neth Milk Dairy J 40:241
- Carlson A, Hill C, Olson N (1987a) Biotechnol Bioeng 29:582
- Horne DS (1989) J Dairy Res 56:535
- Mellema M, Walstra P, van Opheusden JH, van Vliet T (2002) Adv Colloid Interface Sci 98:25
- Ekstrand B, Larsson-Raznikiewicz M, Perlmann C (1980) Biochim Biophys Acta 630:361
- Dalgleish DG, Brinkhuis J, Payens TAJ (1981) Eur J Biochem 119:257
- Ford GD, Grandison AS (1986) J Dairy Res 53:129
- Lieske B (1998) Milchwissenschaftliche 53:562
- Singh H (1995) Heat-induced changes in casein including interactions with whey proteins. In: Fox PF (ed) Heat induced changes in milk. International Dairy Federation, Brussels, pp 86–104
- Pappas C (1992) Lebensm-Wiss Technol 25:102
- Harwalkar V, Kaláb M (1988) Food Microstruc 7:173
- Schreiber R, Hinrichs J (2000) Lait 80:33
- Horne DS (1986) J Colloid Interface Sci 111:250
- Aoki T, Kawahara A, Yoshitaka K, Imamura T (1987) Agric Biol Chem 51:817
- Dong Jang H, Swaisgood H (1990) Arch Biochem Biophys 283:318
- McGann T, Kearney R, Donnelly W (1979) J Dairy Res 46:307
- Kuaye AY (1994) Food Chem 49:207
- Laemmli U (1970) Nature 227:680
- Green MR (1986) J Histochem Cytochem 34:147
- Horne DS (1987) Faraday Discuss Chem Soc 83:259
- Worning P, Bauer R, Øgøndal L, Lomholt S (1998) J Colloid Interface Sci 203:265
- Teixeira J (1986) In: Stanley HE, Ostrowsky N (ed) On growth and form. Netherlands, pp 145
- Holt C, Parker TG, Dalgleish DG (1975) Biochim Biophys Acta 400:283
- Lloset MA, Gugliotta LM, Meira GR (1996) Rubber Chem Technol 69:696
- Gugliotta L, Vega J, Meira G (2000) J Colloid Interface Sci 228:14
- Ambrose Griffin MC, Griffin WG (1985) J Colloid Interface Sci 104:409
- Dalgleish DG (1979) J Dairy Res 46:653
- Carlson A, Hill C, Olson N (1987b) Biotechnol Bioeng 29:590
- Gatti CA, Pires MS (1995) J Dairy Res 62:667
- Queiroz Macedo I, Faro CJ, Pires EM (1993) J Agric Food Chem 41:1537
- Peterson GL (1977) Anal Biochem 83:346
- Darling DF, van Hooydonk ACM (1981) J Dairy Res 48:189
- Dalgleish DG, Horne DS, Law AJR (1989) Biochim Biophys Acta 991:383
- Payens TAJ (1979) J Dairy Res 46:291
- Mc Mahon DJ, Brown RJ (1984) J Dairy Sci 67:919
- Gatti CA, Pires MS, Orellana G, Pereyra J (1996) J Chem Soc Faraday Trans 92:2575
- Braga ALM, Menossi M, Cunha RL (2006) Int Dairy J 16:389
- Slattery CW, Evard R (1973) Biochim Biophys Acta 317:529
- Risso PH, Gatti CA, Zerpa SM, Perez GR (2000) Food Hydrocoll 14:179